Numerical and Experimental Failure Analysis of Deep Drawing with Additional Force Transmission

P. Althaus(✉), J. Weichenhain, S. Hübner, H. Wester, D. Rosenbusch, and B.-A. Behrens

Institute of Forming Technology and Machines (IFUM), Leibniz Universität Hannover, An der Universität 2, 30823 Garbsen, Germany
althaus@ifum.uni-hannover.de

Abstract. Deep drawing is a common forming method, where a sheet metal blank is drawn into a forming die by a punch. In previous research, conventional deep drawing was extended by the introduction of an additional force in the bottom of the cup. The force transmission initiates a pressure superposition in critical areas resulting in a delayed crack initiation. For numerical investigation of the considered process, an accurate modelling of the material failure is essential. Therefore, the parameters of the modified Mohr-Coulomb criterion were identified for the two high-strength steels HX340LAD and HCT600X by means of tensile tests with butterfly specimens. In this research, the fracture modelling is applied in the simulation of deep drawing with and without additional force transmission to enhance the failure prediction. The fracture criterion is validated by experimental deep drawing tests. Finally, the influence of the additional force on the prevailing stress state is evaluated.

Keywords: Sheet metal forming · Deep drawing · Stress-based failure

1 Introduction

Deep drawing is one of the most important manufacturing processes for sheet metal components in the automotive, aerospace and packaging industry. During deep drawing, a sheet metal blank is clamped between a blank holder and a die and formed by a punch. The improvement of deep drawing processes is still the main focus of numerous researches to increase productivity, material utilisation and dimensional accuracy. Furthermore, various possibilities to extend the process limits are being investigated [1]. An extension of the forming limit can be achieved either by strengthening or relieving the force transfer zone in the sheet metal. For a strengthening of the force transfer zone, higher sheet thicknesses or materials with higher tensile strengths can be used [2]. Moreover, locally adapted semi-finished products such as tailored blanks [3] or tailored rolled blanks [4] can be applied to increase the drawing depth.

Relief of the force transmission zone can be achieved by superimposing compressive stresses as this leads to an increased forming capacity of the material. This is already used

M. Liewald et al. (Eds.): WGP 2022, LNPE, pp. 142–151, 2023.
https://doi.org/10.1007/978-3-031-18318-8_15

in forming processes with active media, such as hydro-mechanical deep drawing [5]. Another possibility is the use of a counter punch, which Morishita et al. applied in a deep drawing process with tailored blanks to extend the forming limits [6]. Behrens et al. extended a conventional deep drawing process for the forming of a rectangular cup by using a counter punch, which enables the application of an additional force in the bottom of the cup [7]. Due to the additional force counteracting the forming direction, a pressure-superimposed stress state is created in the bottom and in the transition area from the bottom to the sidewall. The pressure superimposed stress state counteracts the formation of fractures during forming and thus enables an extension of the process window. This was proven in experimental deep drawing tests with two high-strength steels HX340LAD and HCT600 [8]. In a previous study, the forming limit curves of the materials were determined to consider the forming limits in a process simulation. However, necking, which occurs at the radius between the bottom and the sidewall, could not be reliably predicted [9].

In this research, the ductile fracture criterion modified Mohr-Coloumb (MMC) proposed by Bai and Wierzbicki [10] is applied in the process simulation to improve the failure prediction. Peshekodhov et al. proved the suitability of the criterion for a conventional deep drawing process, where cracks occurred in the transition area from the flange to the sidewall [11]. In this work, the criterion is applied to predict the fracture initiation in the bottom radius of the cup during deep drawing with and without additional force transmission. The goal is to improve the fracture modelling in order to fully exploit the potential of this technology for an extension of the process limits. For a validation, experimental deep drawing test are carried out with a special tool setup, which enables the introduction of the additional force in the bottom of the cup.

2 Materials and Methods

2.1 Experimental Setup

For the experimental investigation of deep drawing with additional force transmission and for the validation of the ductile fracture model, experimental tests were carried out. The forming tool shown in Fig. 1 essentially corresponds to the design of a conventional deep drawing tool. This includes the punch, the bottom die and the blank holder.

Additional force was applied to the bottom of the cup by the upper die, which is preloaded by means of a gas pressure spring. A load cell, which is located at the lower end of the punch, allows the punch force to be recorded during the forming process. With the use of a position sensor, force-displacement curves can be evaluated. The tool enables the deep-drawing of rectangular cups in the dimensions of 160 mm x 80 mm and a drawing depth of 55 mm.

The experimental setup was used to determine the process limits regarding the formation of fractures in the deep drawing process with and without additional force transmission as a function of the applied blank holder force. The sheet materials used are HX340LAD+Z (1.0933, short: HX340) and HCT600X-Z100MBO (1.0941, short: HCT600). Both sheet materials are galvanized and have a thickness of 1 mm. First, the sheet metals are cut to size as octagonal blanks. The outer dimensions were 281 mm × 213 mm, corresponding to a deep-drawing ratio of 1.9. The drawing depth of the cups

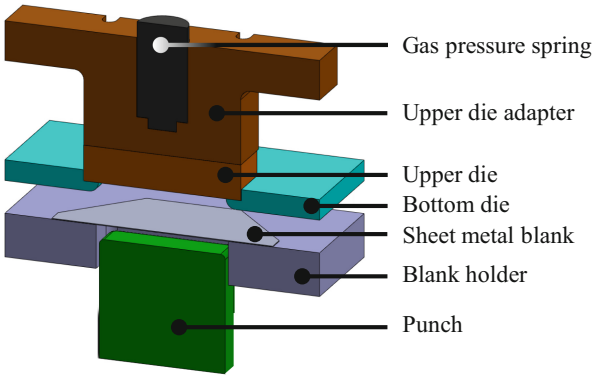

Fig. 1. Tool setup for deep drawing with additional force transmission

was 55 mm and the forming speed was 10 mm/s. In order to ensure uniform tribological conditions, the blanks were lubricated before the deep drawing process with the aid of a spray lubrication system from RAZIOL Zibulla and Sohn GmbH. Raziol CLF 180 was used as the lubricant. The maximum blankholder force at which the components do not fracture was determined both without and with additional force transmission. Therefore, the blank holder force was successively increased in 5 kN steps until a fracture occurred during forming. When a crack appeared, the blank holder force was decreased by 5 kN and the deep drawing was repeated several times. If no crack appeared in five repetitions, the maximum blank holder force was identified. If a crack appeared in the repeated attempts, the blank holder force was again decreased by 5 kN.

2.2 Numerical Validation

For the numerical investigation of the deep drawing process, a simulation model was set up in Abaqus/Explicit, which is shown in Fig. 2 (a). In accordance to the experimental setup, the model consists of the sheet metal, which is clamped between the bottom die and the blank holder, and the forming punch.

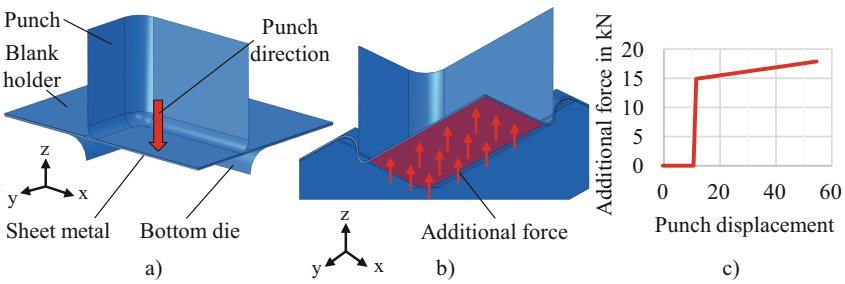

Fig. 2. Numerical simulation model (a) with additional force transmission in form of a pressure field in the bottom of the cup (b) depending on the punch displacement (c)

The simulation was divided into two steps. At first, the force of the blank holder was applied on the sheet metal. Subsequently, deep drawing was carried out by moving the punch with a velocity of 10 mm/s until the final drawing depth of 55 mm is reached. To reduce the computational effort, the symmetry of the process was used and only a quarter of the geometry was depicted.

Instead of the upper die for the additional force transmission, a pressure field is defined at the bottom of the cup. The pressure is activated when the drawing depth of 12 mm is reached. In the real experiment, the force is applied by a gas spring, which is preloaded with 150 bar. This corresponds to an initial force of 15 kN. Due to the increase of pressure in the spring, the force increases to approx. 18 kN at the end of forming (55 mm). The defined pressure field is shown in Fig. 2 (b).

The sheet metal was meshed with solids (C3D8) with an average element edge length of 0.4 mm and three elements across the thickness. The tools were modelled as rigid shells and were also meshed with an element edge length of 0.4 mm. For the sheet materials, elastic-plastic models were defined based on the results of a previous study, where tensile tests were carried out at room temperature according to DIN EN ISO 10002 with the specimens aligned at 0°, 45° and 90° to the rolling direction [7]. The flow curves were extended by means of hydraulic bulge tests for an enhancement of the extrapolation accuracy. For HX340, the approach according to Gosh and for HCT600 a combined approach of Swift and Hocket-Sherby was chosen, because they provided the best approximation to the experimental data. Furthermore, the yield criteria according to Hill was defined for both materials [12]. The flow curves and the yield surfaces with the corresponding parameters are given in Fig. 3.

The failure behaviour of the considered materials was modelled by means of the MMC criterion, which defines the equivalent plastic strain at fracture according to the following equation:

$$\varepsilon_{\mathrm{pl}}^{\mathrm{f}} = \left\{ \frac{A}{c_2} \left[c_{\Theta}^{\mathrm{s}} + \frac{\sqrt{3}}{2-\sqrt{3}} \left(c_{\Theta}^{\mathrm{ax}} - c_{\Theta}^{\mathrm{s}} \right) \left(\sec\left(\frac{\overline{\theta}\pi}{6} \right) - 1 \right) \right] \right\}^{-1/n} \left\{ \left[\sqrt{\frac{1+c_1^2}{3}} \cos\left(\frac{\overline{\theta}\pi}{6} \right) + c_1 \left(\eta + \frac{1}{3} \sin\left(\frac{\overline{\theta}\pi}{6} \right) \right) \right] \right\} \tag{1}$$

Here, the fracture strain is depending on the stress triaxiality η, the normalised Lode angle $\overline{\theta}$ and six material-specific parameters. A and n were identified by fitting the flow curves of the materials to the Swift hardening model. The parameters c_{Θ}^{ax} and c_{Θ}^{s} were left at their default value of 1 analogous to [10]. For the remaining parameters c_1 and c_2, tensile test with butterfly specimens were carried out and simulated in a previous study [13]. The parameters were fitted to the experimental data by reducing the sum of the least squares between experimental plastic strain and predicted plastic strain by the criterion. The resulting parameters are given in Table 1. The corresponding fracture curves are shown in Fig. 4.

For contact between the tools and the sheet metal, “surface to surface” contact was used and coulomb´s law with a friction coefficient of 0.1 was defined for the punch and the blank holder. Since the sheet metal was lubricated on the side to the die, the

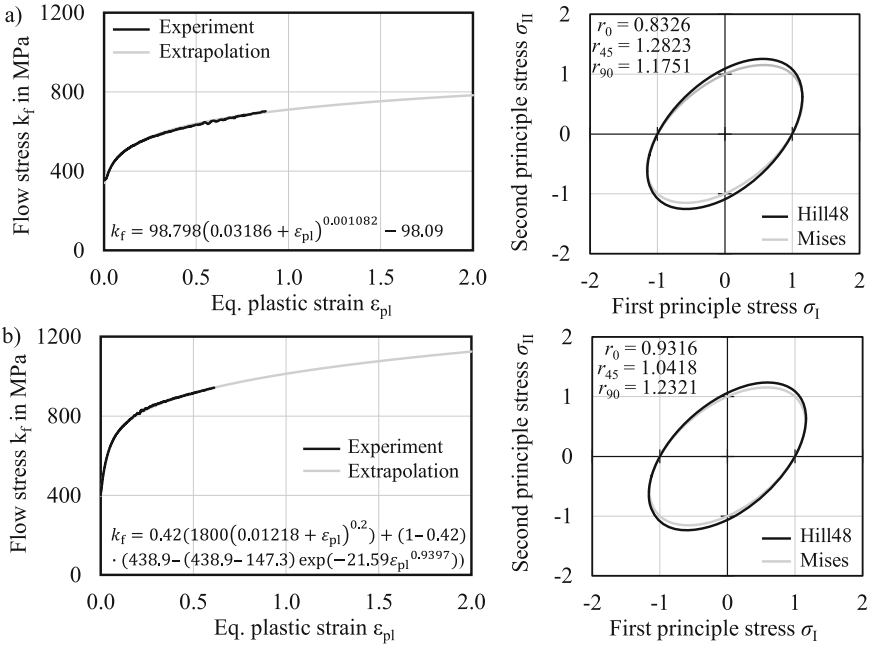

Fig. 3. Flow curves and yield surfaces for HX340 (a) and HCT600 (b) [7]

Table 1. Parameter of the used MMC criterions

	A	n	c_1	c_2
HX340	713.0	0.165	0.208	401.934
HCT600	1018.6	0.143	0.166	560.033

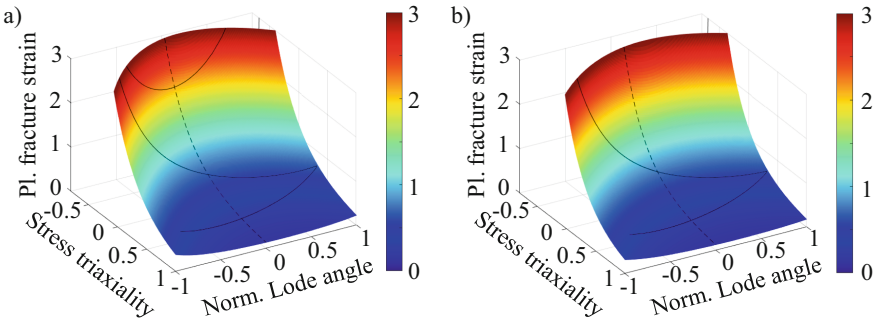

Fig. 4. Plastic fracture strain in the space of stress triaxiality and normalized Lode angle for HX340 (a) and HCT600 (b) based on the MMC criterion

coefficient was reduced to 0.05. To keep the computational effort reasonable, a mass scaling factor of 100 and a time scaling factor of 10 was applied. The application of the scaling factors was tested in an exemplary simulation and showed no significant effect on the results.

3 Results

3.1 Experimental Process Limits

The diagram in Fig. 5 (a) shows the maximum determined blank holder force for deep drawing of HX340 and HCT600. The blank holder force and thus the process window for flawless cups could be increased from 280 to 320 kN for HX340 and from 195 to 230 kN for HCT600 by using additional force transmission. To show the effect of the additional force, exemplary cups made of HX340 are shown in Fig. 5 (b), which were formed with a blank holder force of 320 kN with and without additional force.

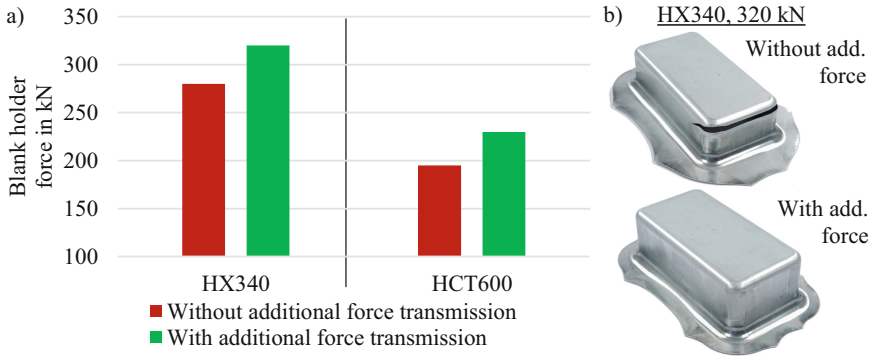

Fig. 5. a) Maximum blank holder force for HX340 and HCT600 and b) cups made of HX340 with a blank holder force of 320 kN with and without additional force transmission.

3.2 Numerical Validation

In Fig. 6, the numerical and experimental force displacement curves are shown for HX340 with Fig. 6 (a) and without Fig. 6 (c) additional force transmission for blank holder forces of 280 and 320 kN. The results of HCT600 are shown in Fig. 6 (b) and Fig. 6 (d) for blank holder forces of 195 and 230 kN. At the beginning of forming, the punch force increases linearly until a drawing depth of approx. 16 mm is reached. Good agreement was achieved by the simulations in the first forming stage. Subsequently, the force measured in the experiments reaches its maximum, followed by a slight decrease until the maximum drawing depth is achieved. In this stage, the force is first overestimated by the simulation, whereas it is underestimated at the end of the forming process. This can presumably be attributed to the fact that a constant friction coefficient is assumed in the simulation, while the friction coefficient is influenced by various factors, such

as contact pressure or the thickness of the lubrication film [14]. Another reason for the deviations could be fluctuations between material batches.

The best agreement with a maximum deviation of 5.70% was achieved by the simulation with HX340 and without the additional force transmission, while the largest maximum deviation of 11.38% occurred in the simulation with HCT600 and without additional force in the bottom of the cup. The activation of the additional force is visible by a sudden increase of the punch force at a drawing depth of 12 mm.

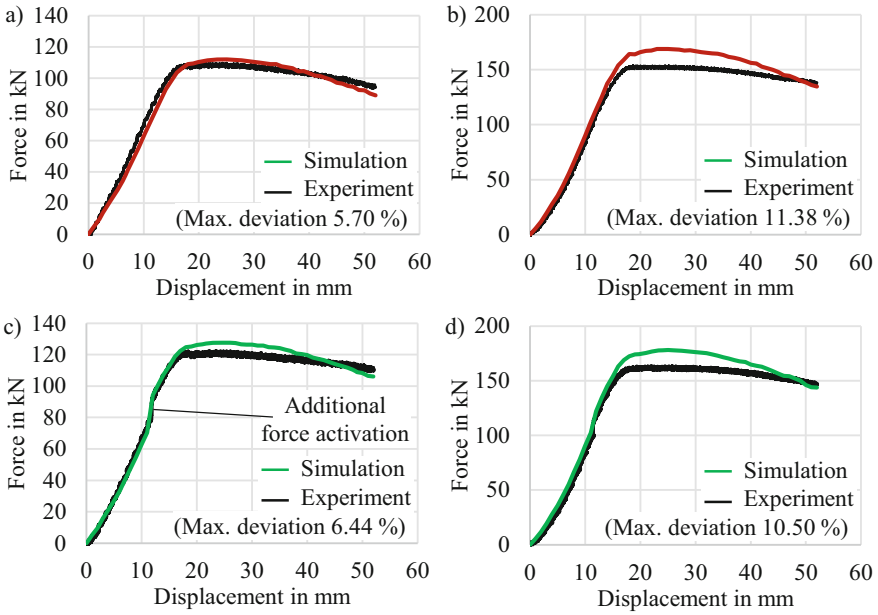

Fig. 6. Force-displacement curves of HX340 with (a) and without (c) additional force as well as HCT600 with (b) and without (d) additional force transmission

In the next step, the prediction accuracy by the MMC criterion was evaluated by comparing the material damage predicted by the simulation to the experimental results without additional force transmission. For HX340, a blank holder force of 320 kN was chosen, because fractures occurred in every experimental test. For HCT600, a corresponding blank holder force of 230 kN was simulated. Figure 7 compares the fractures of the experimental deep drawn cups to the distribution of the damage variable D calculated in the simulation. D is defined according to the following equation:

$$D = \int \frac{d\varepsilon^{\mathrm{pl}}}{\varepsilon_{\mathrm{D}}^{\mathrm{pl}}\left(\eta, \xi(\theta), \dot{\varepsilon}^{\mathrm{pl}}\right)} \tag{2}$$

Here, $\varepsilon_{\mathrm{D}}^{\mathrm{pl}}$ is the equivalent plastic strain at the onset of fracture according to the MMC criterion. It depends on the stress triaxialty η, the plastic strain rate $\dot{\varepsilon}^{\mathrm{pl}}$ and the third stress invariant ξ, which is depended on the Lode angle. Material damage is present,

when D reaches or exceeds the value of one. As shown in Fig. 7 (b) for HX340 and Fig. 7 (d) for HCT600, the MMC criterion predicts the initiation of a fracture in the radius at the bottom of the cup. This shows a good agreement regarding the location of the fractures in the experiments. In comparison to the simulation, the experimental deep drawn cups show more progressed cracks, which are present along the entire width of the cups. This crack propagation is not represented by the simulation, since no damage evolution or element removal is taken into account. A comparison of the exact time of fracture initiation difficult, because the experiments had to be stopped manually, when a fracture occurred. Due to the fast processing speed, it was not possible to stop the punch right in time of the fracture initiation. Furthermore, it can be noticed that in the simulations material damage also accumulates in the corner of the sidewall. However no fractures develop in this section, which is in accordance to the experiments. Therefore, the MMC criterion is considered to be well suited for the prediction of fractures in the bottom of the cups during deep drawing.

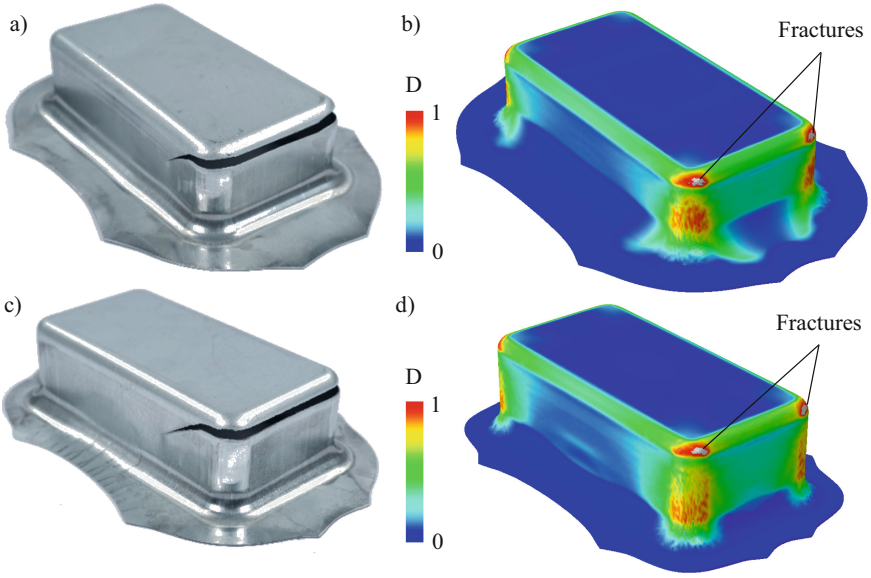

Fig. 7. Experimental and numerical fracture initiation for HX340 (a, b) and HCT600 (c, d)

Subsequently, the simulations shown in Fig. 7 were carried out with the additional force by activating the pressure field in the bottom of the cup. The distribution of the damage variable D is shown in Fig. 8 (a) for HX340. It can be seen, that no fractures are predicted in the simulation with additional force transmission, which is in accordance to the experimental results. For a better understanding of the effect of the additional force, the equivalent plastic strain and the stress triaxiality are evaluated at five element in the radius of the cup, where fractures occurred without the additional force. The averaged values of the elements are shown in Fig. 8 (b) for HX340 and in Fig. 8 (c) for HCT600.

Due to the pressure superposition, the stress state shifts to lower stress triaxialities. Thus allowing higher plastic strains to be reached before material failure occurs.

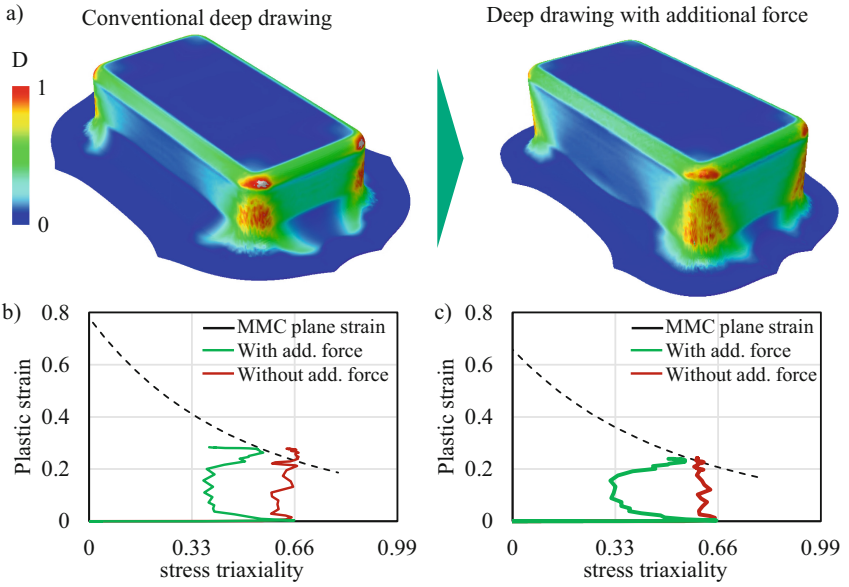

Fig. 8. Simulation results for HX340 without and with additional force transmission (a) and evolution of the plastic strain over stress triaxiality for HX340 (b) and HCT600 (c)

4 Conclusion and Outlook

This contribution deals with the investigation of an extended deep drawing process, where an additional force is applied in the bottom of the cup by a preloaded upper die. Experimental deep drawing test were carried out with the high-strengths steels HX340 and HCT600 under a variation of the blank holder force to identify the process limits regarding fractures in the bottom of the cup. It was found, that the maximum blank holder forces of 280 kN for HX340 and 195 kN for HCT600 could be extended by the additional force transmission to 320 kN and 230 kN, which corresponds to an increase of 14.3% and 17.9%, respectively. Due to the increase of the maximum blank holder force, larger deep drawing ratios can be realised, thus an extension of the process window has been achieved.

Numerical simulations were carried out to predict the material failure by the application of the MMC criterion. The fracture criterion showed good agreement to the experimental results regarding the location of the fracture initiation. Furthermore, the extension of the process limits due to the additional force transmission was successfully considered. The delayed fracture initiation could be attributed to lower stress triaxialities in the bottom radius of the cup, resulting in higher tolerable fractures strains.

Acknowledgements. The results presented were obtained in the project "Extension of the forming limits during deep drawing by additional force transmission" – 212270168. The authors thank the German Research Foundation (Deutsche Forschungsgemeinschaft, DFG) for their financial support.

References

1. Wifi, A., Abdelmaguid, T., El-Ghandour, A.: A review of the optimization techniques applied to the deep drawing process. In: 37th International Conference on Computers and Industrial Engineering (2007)
2. Kumar, D.R.: Formability analysis of extra-deep drawing steel. J. Mater. Process. Technol. **30–131**, 31–41 (2002)
3. Merklein, M., Maren, J., Lechner, M., Kuppert, A.: A review on tailored blanks—production, applications and evaluation. J. Mater. Process. Technol. **214**(2), 151–164 (2014)
4. Meyer, A., Wietbrock, B., Hirt, G.: Increasing of the drawing depth using tailored rolled blanks—numerical and experimental analysis. Int. J. Mach. Tools Manuf. **48**(5), 522–531 (2007)
5. Zhang, S.H., Danckert, J.: Development of hydro-mechanical deep drawing. J. Mater. Process. Technol. **83**(1–3), 14–25 (1998)
6. Morishita, Y., Kado, T., Abe, S., Sakamoto, Y., Yoshida, F.: Role of counterpunch for square-cup drawing of tailored blank composed of thick/thin sheets. J. Mater. Process. Technol. **212**(10), 2102–2108 (2012)
7. Behrens, B.-A., Bonk, C., Grbic, N.,Vucetic, M.: Numerical analysis of a deep drawing process with additional force transmission for an extension of the process limits. IOP Conf. Ser. Mater. Sci. Eng. **179**(1), 012006 (2017)
8. Behrens, B.-A., Bouguecha, A., Bonk, C., Grbic, N., Vucetic, M.: Validation of the FEA of a deep drawing process with additional force transmission. AIP Conf. Proc. **1896**(1), 080024 (2017)
9. Behrens, B.-A., Bouguecha, A., Bonk, C., Rosenbusch, D., Grbic, N., Vucetic, M.: Influence of the determination of FLC's and FLSC's and their application for deep drawing process with additional force transmission. In: Proceedings of 5th International Conference on Advanced Manufacturing Engineering and Technologies, pp. 405–417 (2017)
10. Bai, Y., Wierzbicki, T.: Application of the extended Coulomb-Mohr model to ductile fracture. Int. J. Fract. **161**(1), 1–20 (2010)
11. Gladkov, Y., Peshekhodov, I. A., Vucetic, M., Bouguecha, A., Behrens, B.-A.: Implementation of the Bai & Wierzbicki fracture criterion in QForm and its application for cold metal forming and deep drawing technology. In: MATEC Web of Conferences, vol. 21, pp. 12009 (2015)
12. Hill, R.: A theory of the yielding and plastic flow of anisotropic metals. Proc. Roy. Soc. Lond. **193**(1033), 281–297 (1984)
13. Behrens, B.-A., Rosenbusch, D., Wester, H., Althaus, P.: Comparison of three different ductile damage models for deep drawing simulation of high-strength steels. In: IOP Conference series. Materials Science and Engineering. 1238 012021 (2022)
14. Merklein, M., Zöller, F., Sturm, V.: Experimental and numerical investigations on frictional behaviour under consideration of varying tribological conditions. In: Advanced Materials Research, vol. 966–967, pp. 270–278 (2014)